Behavior of storm-induced suspension interflow in subtropical Feitsui Reservoir, Taiwan

Yi-Jing Cherry Chen[1] and Shian-Chee Wu
Graduate Institute of Environmental Engineering, National Taiwan University, Taipei 106, Taiwan, Republic of China

Bing-Shiou Lee and Chang-Che Hung
Taipei Feitsui Reservoir Administration, Taipei 106, Taiwan, Republic of China

Abstract

A storm-induced suspension interflow (a kind of turbidity current) in subtropical deep (113-m maximum depth) Feitsui Reservoir, Taiwan, was traced and simulated for both water quantity and quality control. To trace the path of the turbidity current, the spatial and temporal distributions of water temperature, turbidity, and concentration of total phosphorus were obtained weekly from seven sampling sites at 10-m intervals vertically. These were obtained to trace the path of the turbidity current. A hydrodynamic model simulation agreed closely with the observations. Thermal stratification of the water column was disrupted by storms. After plunging into the reservoir, the suspension interflow resulting from higher concentrations of the suspended solids and lower water temperature moved horizontally toward the dam at depths of 50–60 m. Adjusting the location of subsurface withdrawal accordingly reduced the intake of suspended solids and total phosphorus associated with the turbidity current. Some of the suspended solids in the lower layer might still affect the surface water quality through vertical mixing, especially when thermal stratification is disturbed.

Water inflows contribute to mixing within lakes and reservoirs and are also important sources of dissolved and particulate materials. The extent of mixing or dissipation of inflow in a lake or reservoir is controlled primarily by the magnitude of the inflows and their density. Density currents are formed when inflowing water is denser than the surface water (Chikita 1989; Martin and McCutcheon 1999), which may flow into the downstream reservoir regions along the beds or form interflows.

The density difference between the water body and the inflowing water may result from differences in temperature, suspended solids content, dissolved solids content, salt concentration of the fluids, or from some combination of these differences (Alavian et al. 1992; Jiahua 1986). Turbidity currents are flows containing excess quantities of suspended fine solid material, which causes the dense water to plunge to a subsurface level in lakes or reservoirs (Simpson 1987). Field observations of density currents or turbidity currents have been conducted in numerous lakes or reservoirs: Lake Ogawara in Japan (Dallimore et al. 2001), the Katsyrazawa Reservoir in Japan (Chikita 1989), Lake Geneva in Switzerland (Lambert and Giovanoli 1988), the Sanmenxia and Guantinh Reservoirs in China (Jiahua 1986), Lake Ouachota and Fayetteville Green Lake in the United States (Ludlam 1974; Ford and Johnson 1986), and the Alpine Luzzone Reservoir in Switzerland (De Cesare et al. 2001). Although the density gradient of turbidity currents is favored by heavily silt-laden rivers (Jiahua 1986), measured suspended solids concentration of the sediment-laden Rhone River flowing into Lake Geneva also shows that quite low concentrations of suspended solids (<1 g L^{-1}) are sufficient to generate turbidity currents (De Cesare et al. 2001). Depending on the density difference between the inflows and ambient waters, the density currents in reservoirs can flow into the downstream area with overflow, underflow, and interflow types (Martin and McCutcheon 1999). If underflows are denser than bottom waters, they may remain on the bottom. If they are less dense than the bottom most layer, the underflow separates from the bottom as an interflow. For a complete review of gravity currents, please read Simpson (1987) and Kneller and Buckee (2000).

Density currents may transport undesirable materials such as suspended solids, organic chemicals, or nutrients from the watershed to downstream reservoir regions (Nix 1981; Wetzel 2001) or may cause sedimentation (Annandale 1987; De Cesare et al. 2001). Appropriate reservoir operation to avoid sedimentation or water quality deterioration requires knowledge of density current behavior. A cold water density current in the winter supplies oxygen to the hypolimnion in the deep subtropical Feitsui Reservoir in Taiwan (Chen and Wu 2003). In August 1996, a turbidity current was observed in Feitsui Reservoir after a typhoon. This turbidity current formed a stable submerged horizontal layer at a depth of 30 m containing high suspended solids concentrations, and it stayed behind the dam for 4 months. It carried up to 71% of the annual suspended solids loading, caused serious sedimentation, and reduced available reservoir volume. A high amount of polyaluminum chloride was required to reduce turbidity of raw water in the drinking water treatment process. Improved knowledge of the formation of turbidity cur-
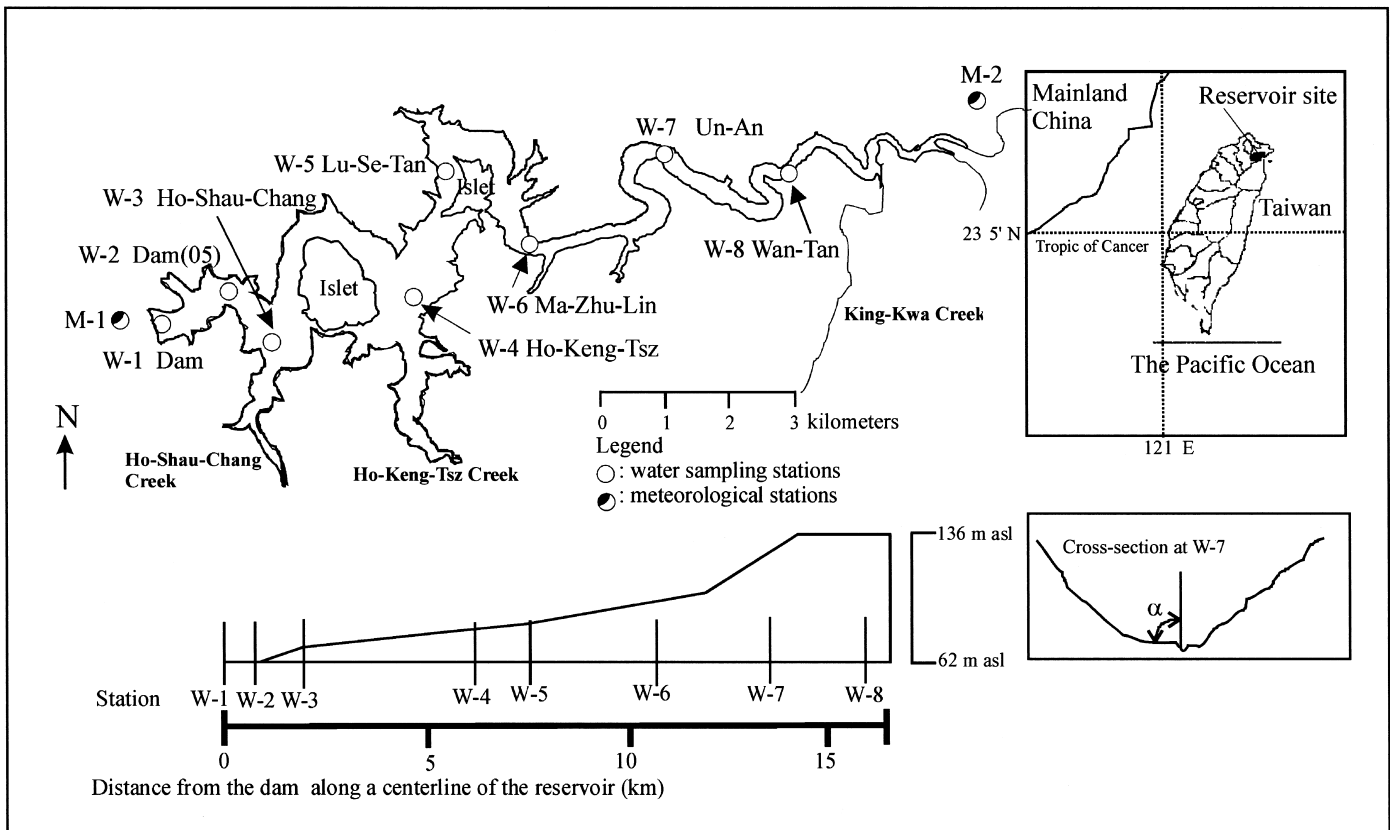

Fig. 1. Location of Feitsui Reservoir and the stations to observe water quality and hydrological parameters.

rents, especially the plunge point and depth of these currents in such subtropical and deep water bodies, is essential for reducing their influence on both the water quantity and water quality.

We performed detailed field observations following a storm event that caused high precipitation in the watershed of Feitsui Reservoir in 2001. The data obtained were used to (1) study the transport process of the turbidity current by tracing spatial and temporal variations of the concentration of suspended solids in the reservoir; (2) compare a predicted behavior of the turbidity current, based on the Hebbert et al. (1979) analytical solutions of the formation of the density currents, with the observed data; (3) assess the benefits of reducing the accumulation of high suspended solids and total phosphorus carried by the turbidity current by adjusting the location of the subsurface withdrawal; and (4) obtain the vertical profile of suspended solids and water temperature during a cold front event to analyze the stability of the water body.

Materials and methods

Site background—Feitsui Reservoir, located downstream of Peishih Creek (24°9′N, 121°6′E) and completed in 1987, is the major water source for over 4 million people living in the Taipei metropolis and suburbs in northern Taiwan (Fig. 1). The designed total water storage capacity of the reservoir is 406×10^6 m^3, and its surface area is 10.24 km^2. The main

stream, Peishih Creek, has a meandering morphology and is 21 km long. The three tributaries (King-Kwa Creek, Ho-Keng-Tsz Creek, and Ho-Shau-Chang Creek) account for <25% of the total inflow. The mean depth of the reservoir is 39.7 m, and the maximum depth is 113.5 m at the dam; the normal maximum water surface elevation is 170 m above sea level (asl). Three water intakes are located near the dam at depths of 15 m (148 m asl), 35 m (128 m asl), and 55 m (108 m asl). The average gradient of the reservoir bed is 0.3%. In 2001, the average total water storage capacity of the reservoir was 298.9×10^6 m^3, and the yearly total outflow was 948.8×10^6 m^3. The average water residence time of the reservoir in 2001, estimated by subdividing the water volume by the outflow, was 115 d.

Feitsui Reservoir is located in an area with a subtropical oceanic climate, and its annual mean air temperature is between 18°C and 23°C from 1991 to 2001. Typhoons bring huge amounts of water in the summer and autumn, whereas monsoons bring cold fronts with abundant precipitation in the winter. The mean annual precipitation is 3,765 mm from 1991 to 2001, with abnormal increases of annual precipitation in 1998, 2000, and 2001. In September 2001, during typhoons Nari (13–19 September 2001) and Lekima (23–28 September 2001), the total precipitation was 1,666 mm, corresponding to 32% of the total precipitation during that year. The total inflow into the reservoir during these storm events exceeded 508×10^6 m^3, and serious soil erosion occurred throughout the watershed.

Table 1. The dimension of the cross-sections at the water sampling stations.*

Site	Distance from the dam along a centerline (km)	Cross-section area (m²)	Depth (m)	Width (m)	Hydraulic depth (m)
W-1	0	22,811	100	385.2	50
W-2	1.67	24,423	90	385.5	45
W-3	2.24	61,753	80	945.2	40
W-4	6.37	32,559	80	613.9	40
W-5	7.62	6,629	60	141.6	30
W-6	10.82	16,011	50	541.2	25
W-7	13.50	4,368	20	220	10

* The estimated data is based on the normal maximum water level (170 m asl) at dam.

Water sample collection and analysis—Field investigations began 27 September 2001, just after Typhoon Lekima left the area. Our measurements were planned for a 3-month period (September–December 2001) and were designed to verify the long-term effect of turbidity currents on the water quality. Water samples were collected weekly at 10 m depth intervals at sampling sites W-1 (Dam), W-2 (Dam [05]), W-3 (Ho-Shau-Chang), W-4 (Ho-Keng-Tsz), W-5 (Lu-Se-Tan), W-6 (Ma-Zhu-Lin), and W-7 (Un-An; Fig. 1). The distance from the dam along a centerline of the reservoir, the cross-sectional area, and the width and depth of each sampling site in relation to the normal maximum water level as 170 m (asl) are listed in Table 1. Turbidity, water temperature, transparency, and total phosphorus (assumed to be carried with the absorption to suspended solids) were monitored to track a turbidity current.

Turbidity was measured using a portable turbidity meter (HACH 2100P). Water temperature was measured by a portable conductivity/temperature meter (YSI 30). A linear regression equation relating the suspended solids concentration, C_{SS}, to the turbidity based on eight samples was used to convert the turbidity (Nephelometric Turbidity Unit, NTU) to the concentration of suspended solids (milligrams per liter [mg L^{-1}]; $R = 0.9961$):
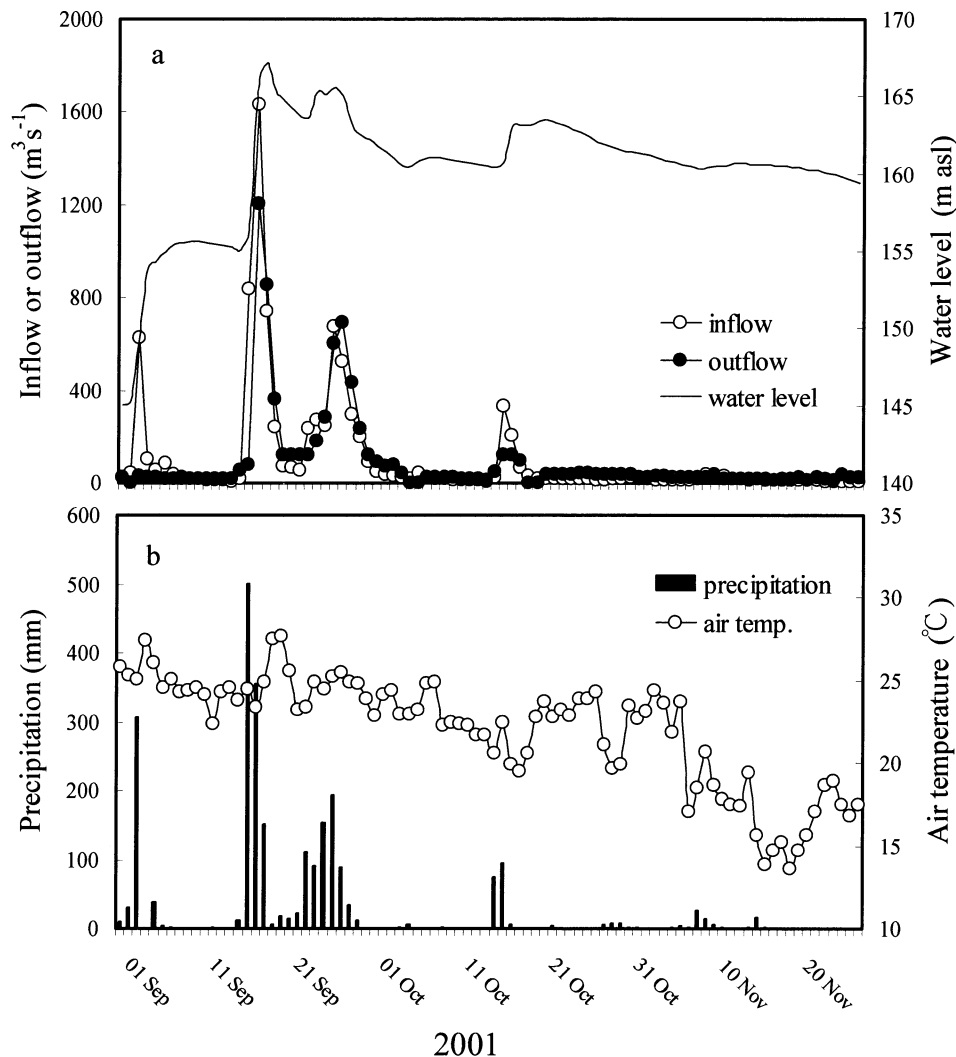

Fig. 2. Hydrograph of the storm. (a) Measured inflow, outflow, and water level. (b) Precipitation and air temperature.
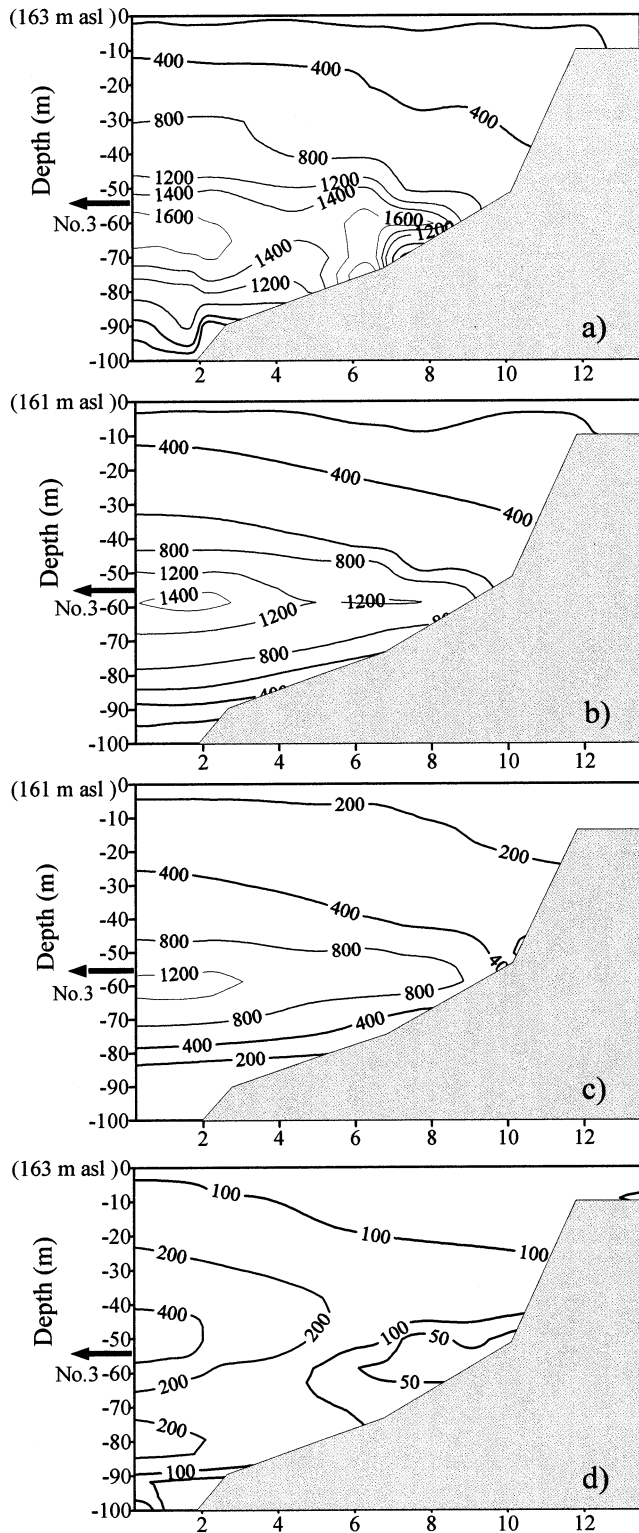
Fig. 3. Spatial and temporal distributions of the suspended solids (SS; mg L^{-1}) in Feitsui Reservoir: (a) 28 September 2001 (0 d after the storms); (b) 2 October 2001 (4 d after the storms); (c) 8 October 2001 (10 d after the storms); (d) 31 October 2001 (33 d after the storms). The No. 3 subsurface withdrawal (108 m asl) was used to discharge the excess suspended solids loading. See Fig. 1 for the locations of the water sampling sites.

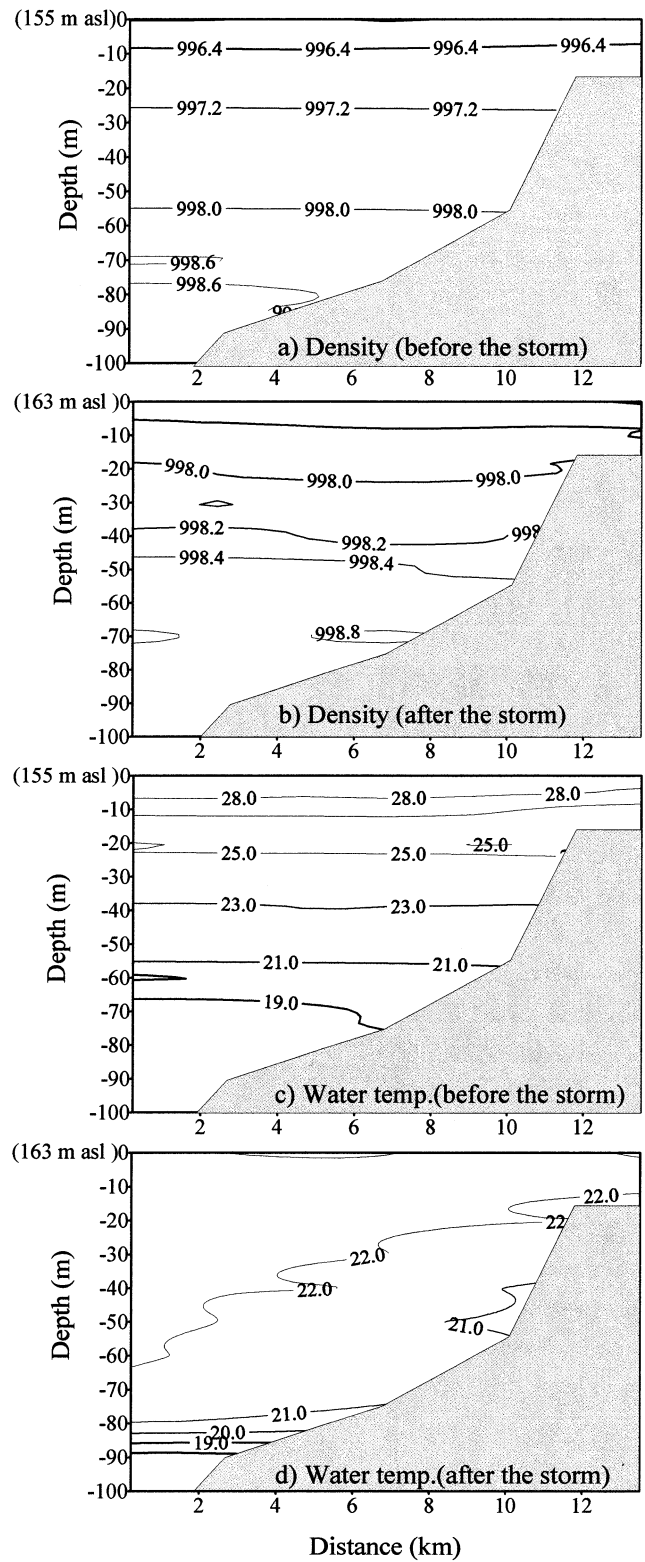Fig. 4. Isopleths of the (a, b) density of water (kg m^{-3}) and (c, d) water temperature (°C) in Feitsui Reservoir before and after the storms. The sampling dates before and after the storms were 6 September 2001 and 18 October 2001, respectively.

Table 2. Parameters specified in the analytical solutions for the turbidity currents.

Parameter	Value	
Internal Froude number of the inflow, F_i	0.238	Eq. 2
Froude number at the location of the plunge, F_p	0.238	Eq. 6
Bed friction, f_b	0.03 (assumed)	
Interfacial friction coefficient, f_i	0.004 (assumed)	
Slope of the reservoir bed, S_0	0.003 (measured)	
One-half base angle of a triangular cross-section, α	70.5° (measured)	
Averaged peak flow, Q (m³ s⁻¹)	497.2	13 Sep to 19 Sep
Inflow velocity, u (m s⁻¹)	0.12	
Hydraulic depth of the inflow, h_o (m)	44.8	Eq. 7
Total density of the inflow, ρ (kg m⁻³)	998.4	
Difference between the densities of the inflow and the receiving water, $\Delta\rho$ (kg m⁻³)	1.22	Eqs. 3–5
Specific gravity of suspended solids, SG	2.65 (assumed)	
Entrainment coefficient, E	7.3 × 10⁻⁴	Eq. 8
Coefficient that parameterizes the efficiency of the boundary-introduced turbulent kinetic energy, C_k	1.9 (assumed)	Hebbert et al. (1979)
Bottom drag coefficient, C_d	0.008	($C_D = [f_b + f_i]/4$)
Location of the plunge point, x (km; upstream of the dam along the centerline)	6.0	Eqs. 9–10

$$\text{Turbidity (NTU)} = 0.402 \times C_{SS} \text{ (mg L}^{-1}\text{)} \quad (1)$$

The concentration of total phosphorus was determined using the ascorbic acid method of Murphy and Riley (1962). Transparency and light attenuation were measured with a 30 cm diameter Secchi disk.

Hydrological and meteorological conditions, including water level, air temperature, precipitation, and outflow rate of the reservoir during storm events were continuously measured at stations M-1 and M-2 (Fig. 1), respectively, with an automatic stage recorder, a temperature recorder, a remote sensing rain gauge system, and a flow meter. Water inflow was estimated based on the water level-inflow histogram.

Analysis of turbidity currents—Generally, in the case of a dense inflow entering a reservoir, the flow width increases with distance downstream from the river inlet and the plume would be three-dimensional as the result of vertical/lateral dispersion and mixing, variation cross sections, and entrainment between the inflow and the ambient waters. The important density current parameters (i.e., propagation speed, thickness, and the point of plunging) can be used to determine a change in water quality at different depths (Alavian et al. 1992). By means of a simple normal flow theory, we used the simplified one-dimensional model of Hebbert et al. (1979) to estimate the location and depth of a plunge point and underflow in the triangular, river-shaped Feitsui Reservoir. Three-dimensional effects along the long and meandering stream were ignored. The location of the plunge point of the turbidity current was estimated by assuming that the internal Froude number of the inflow (F_i) equals the Froude number at a plunge point (or separation point; F_P):

$$F_i^2 = \frac{u^2}{g\frac{|\Delta\rho|}{\rho}h_0} = F_P^2 \quad (2)$$

where u is the inflow velocity, g is the gravitational acceleration, h_0 is the hydraulic depth of the inflow, ρ is the bulk density of the inflow, and $\Delta\rho$ is the difference between the densities of inflow and receiving water in the reservoir. The density function, developed by Gill (1982) and Ford and Johnson (1983), is

$$\rho = \rho_{T_W} + \Delta\rho_S \quad (3)$$

$$\rho_{T_W} = 999.8452594 + 6.793952 \times 10^{-2}T_W$$
$$- 9.095290 \times 10^{-3}T_W^2$$
$$+ 1.001685 \times 10^{-4}T_W^3 - 1.120083 \times 10^{-6}T_W^4$$
$$+ 6.536332 \times 10^{-9}T_W^5 \quad (4)$$

$$\Delta\rho_S = C_{SS}\left(1 - \frac{1}{SG}\right) \times 10^{-3} = 0.00062C_{SS} \quad (5)$$

where ρ_{T_W} is the density of water as a function of temperature (T_W), $\Delta\rho_S$ is the density increment owing to the concentration of suspended solids (C_{SS}), and SG is the specific gravity of suspended solids (assumed to be 2.65).

The cross-section of the waterway in Peishih Creek, the main stream into Feitsui Reservoir, has a near-triangular shape from sites W-5 to W-8 (*see* Fig. 1). A triangular cross-section with a one-half base angle $\alpha = 70.5°$ and a bed slope of $\tan(\phi) = 0.003$ measured at site W-7 was used in a sample case. The hydraulic depth was half of the total depth. The area of this triangular cross section was $A = h_0^2\tan(\alpha)$. If a triangular cross section of constant width is assumed, and recalling that $u = Q/A$, solving Eq. 2, the hydraulic depth, h_o, results in (Hebbert et al. 1979)

$$h_0 = \left[\frac{2Q^2}{F_i^2\frac{g|\Delta\rho|}{\rho}\tan^2(\alpha)}\right]^{1/5} \quad (6)$$

The Froude number, F_P, can be determined as follows (Hebbert et al. 1979):

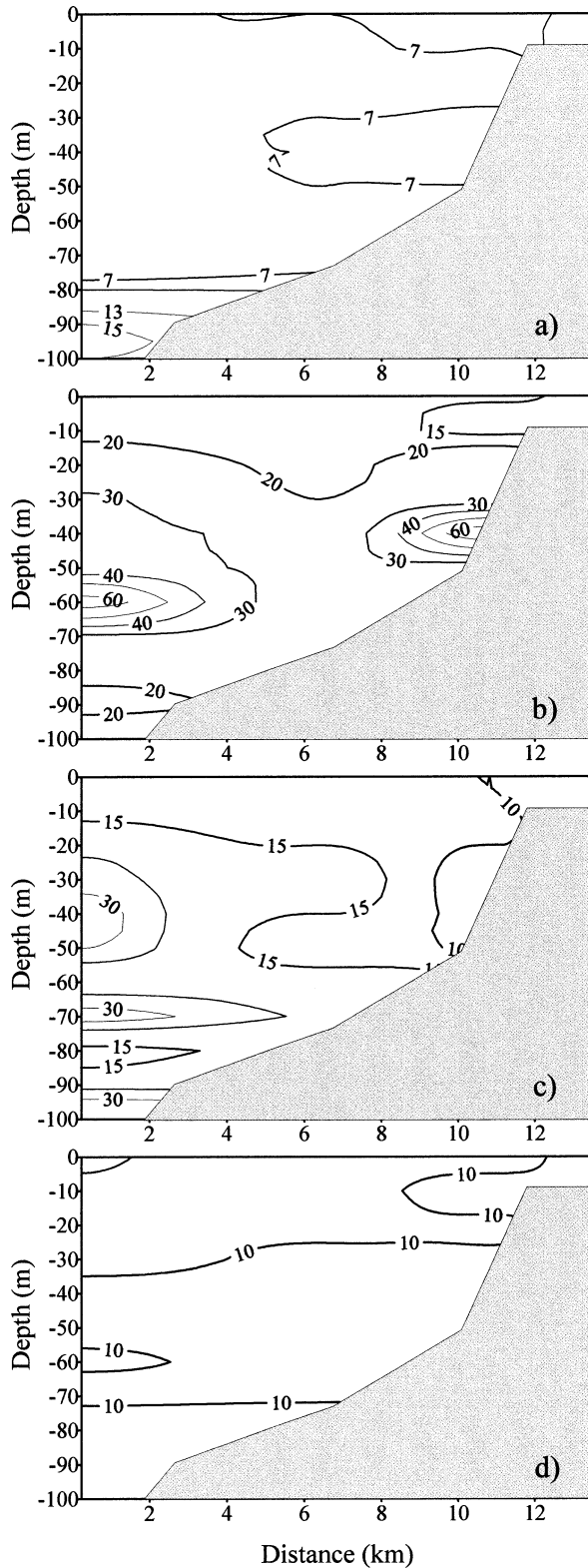$$F_P^2 \approx \frac{\sin(\alpha)\sin(\phi)}{C_D}[1 - 0.53C_kC_D^{0.5}\sin(\alpha)] \quad (7)$$

Fig. 5. The spatial distributions of the concentrations of total phosphorus (TP) (μg L^{-1}) before and after the storms: (a) 8 August 2001 (1 month before the storms), (b) 3 October 2001 (5 d after the storms), (c) 7 November 2001 (40 d after the storms), and (d) 5 December 2001 (68 d after the storms).

where C_D is the dimensionless bottom drag coefficient ($C_D = (f_b + f_i)/4$), f_b is the bed friction coefficient, f_i is the interfacial friction coefficient, and C_k is a coefficient parameterizing the efficiency of the boundary-introduced turbulent kinetic energy. Hebbert et al. (1979) discussed field and laboratory values of C_k and found that this parameter was a universal constant, with a value $C_k = 1.9$.

Mixing and entrainment following the plunge of the inflow are caused by bottom shear and shear across the surface of the underflow. The entrainment coefficient, E, the normal depth of the underflow along the centerline, h_u, and the increase in flow due to entrainment in a triangular cross-section were calculated as (Hebbert et al. 1979)

$$E = \frac{1}{2}C_k C_D^{3/2} F_P^2 \tag{8}$$

$$h_u = \frac{6E}{5}x + h_{u0} \tag{9}$$

where x is the distance downstream from the plunge point, and h_{u0} is the initial thickness of the underflow, which is approximately equal to the depth at the plunge point. The flow increased by entrainment, $Q(x)$, is

$$Q(x) = Q_P\left[\left(\frac{h_u}{h_i}\right)^{5/2} - 1\right] \tag{10}$$

where Q_P is the flow rate at the plunge point, and h_i is the depth at the previous calculation step. The dissipation of suspended solids as well as the water temperature during entrainment could reduce the density of the turbidity currents. Equations 9 and 10 then were solved iteratively. The predicted values using this analytical method are compared with the monitored plume of suspended solids.

Results and discussion

Occurrence of turbidity currents—Two major storms in September 2001 (Fig. 2) brought 1,666 mm of precipitation. The peak inflow associated with typhoon Nali (13–19 September 2001) reached 1,631 m^3 s^{-1} on 17 September. The peak inflow associated with typhoon Lekima (23–28 September 2001) was 676 m^3 s^{-1} on 26 September. Figure 3a–d illustrates the spatial and temporal variations of suspended solids in the reservoir. Immediately after the storm, the peak concentration of suspended solids was 2,056 mg L^{-1} (turbidity 826 NTU) at a depth of 80 m at location W-4 (Ho-Keng-Tsz), which was 6.37 km upstream of the dam (Fig. 3a). With respect to the movement of the turbidity in the reservoir, it was speculated that a suspension interflow (a subset of turbidity currents) had formed, which moved horizontally toward the dam at depths of 50–60 m. The concentration of suspended solids behind the dam between 50 and 60 m ranged from 1,364 to 1,733 mg L^{-1}.

Figure 4 shows the density and water temperature before and after the storm. Before the storm event (6 September 2001), thermal stratification was stable throughout the water body. On 18 October 2001, 10 d after the storm event, the density of water below 50 m was homogeneous and greater than in the upper layer (Fig. 4b), indicating that heat and

Table 3. A comparison of the approach by selecting either No. 1 or No. 3 withdrawal to discharge the suspended solids (SS) loads in the reservoir.*

Period (in 2001)	Daily outflow 10^6 m³ day⁻¹	Total outflow 10^6 m³	No. 1, 148 m asl		No. 3, 108 m asl	
			SS conc. (mg L⁻¹)	SS loading ($\times 10^3$ kg)	SS conc. (mg L⁻¹)	SS loading ($\times 10^3$ kg)
27 Sep–01 Oct	6.3	31.7	622	19,712	2,041	64,656
02 Oct–07 Oct	3.2	17.1	398	7,597	1,369	23,376
08 Oct–17 Oct	3.2	31.8	361	11,475	1,195	37,985
18 Oct–24 Oct	2.7	19.0	241	4,596	996	18,952
25 Oct–30 Oct	3.5	21.1	236	4,980	697	14,679
31 Oct–06 Nov	3.5	24.6	224	5,505	622	15,291
07 Nov–11 Nov	2.3	11.4	137	1,559	488	5,557
12 Nov–20 Nov	1.6	14.0	187	2,621	274	3,844
Sum of the SS removed (by weight)				58,045		187,077
(by volume)				44,650[b]		143,906[a]
Excess discharge of SS by adjusting the location of withdrawal from No. 1 to No. 3 (a–b)						99,256 (m³)

* The specific weight (ρ) of the sediment, 1.3, was used to estimate the volumetric SS loads. conc., concentration.

mass of the bottom water were thoroughly mixed. The inflow was denser than surface water in the reservoir because of higher concentrations of suspended solids and lower water temperature (23.8°C). However, the density of the turbid flow was less than that of the bottom water, resulting in the suspension interflow at a depth between 50 and 60 m (Figs. 3 and 4). The monitored turbidity current was suggested as the interflow type, a subset of the turbidity currents.

Suspended solids did not accumulate as sediment at W-4 (x = 6.37 km) as described by Yu et al. (2000), where a turbidity current hit the dam construction, causing it to reflect back in the direction of flow (90° to the obstruction) and resulting in mud deposition. Because of the long distance (6.37 km) between the dam and site W-4 in Feitsui Reservoir, it is doubtful that this occurred here. The width of the main stream in the reservoir increased gradually from 142 m at W-5 (x = 7.62 km) to 614 m at W-4 (x = 6.37 km) along the centerline (see Table 1). The cross-sectional area of site W-4 is 32,559 m², about 4.9 times larger than that of site W-5. The estimated longitudinal velocity at site W-4 decreased sharply, which caused suspended solids to settle and accumulate. The changing morphology of the basin was one of the reasons for large sedimentation of suspended solids at site W-4.

Predicting the path of the turbidity current using the analytical solutions—Equations 1–10 were used to predict the path of the turbidity current. Table 2 lists the parameters used in the hydrodynamic model with average peak flow during typhoon Nari (13–19 September 2001) of 497.2 m³ s⁻¹. The hydrological conditions in Fig. 2 were utilized. The average inflow water temperature was 23.8°C. Based on the measured suspended solids concentration immediately after the storms (Fig. 3a), the inflow suspended solids concentration was assumed to be 1,600 mg L⁻¹, which was the concentration at a depth of 50 m near the dam. The estimated total density of the inflow including the density increment due to suspended solids was 998.4 kg m⁻³. The receiving water temperature was 24.5°C before the storm, and the density

difference between the inflow and receiving water was 1.22 kg m⁻³.

For the triangular longitudinal cross-sections of the reservoir, the hydraulic depth was one half of the total depth. The Froude number, F_P, of the flow was estimated to be 0.238, and the estimated hydraulic depth (h_o) of the plunge point was 39 m, which is close to the observed hydraulic depth, 40 m at W-4 (x = 6.37 km) in Table 1. The plunge point of the turbidity current should be near location W-4 (x = 6.37 km). The entrainment coefficient, E, was 0.00073. If the initial thickness of the turbid flow, h_{u0}, is assumed to equal the depth at the plunge point, h_0, the greatest depth (h_u) that would have been reached by the turbid flow after numerical iterations of Eqs. 9 and 10 was estimated to be 52.3 m at x = 6.0 km with iteration error smaller than 5%. The estimated thickness of the suspension interflow, 52.3 m, was a bit shallower than the observed depth, 55 m (mean value of 50 and 60 m), shown in Fig. 3. The simulation result is thus consistent with the observed data.

Strategy for reducing suspended solids and total phosphorus loading—Fine particles are not only an aesthetic problem, but also carry nutrients such as phosphorus (P), creating water quality control problems (Savenko 1999; Uusitalo et al. 2000; Chen and Wu 2004). Particle-bound P comprises over 65% of total phosphorus in the surface runoff of the Feitsui watershed (Chen and Wu 2004). The spatial distributions of the concentrations of total phosphorus before and after the storm are illustrated in Fig. 5. Before the storm (8 August 2001), the average concentration of total phosphorus in the reservoir was around 7.0 μg-P L⁻¹ (Fig. 5a). After the storms, two clusters of high total phosphorus were found (Fig. 5b), one at the depth of 60 m near the dam, the other at the depth of 40 m near site W-6 (x = 10.8 km). The peak concentrations of total phosphorus of the two clusters were 65 and 68 μg-P L⁻¹, respectively. The transport path of total phosphorus was similar to that of suspended solids (Fig. 3).

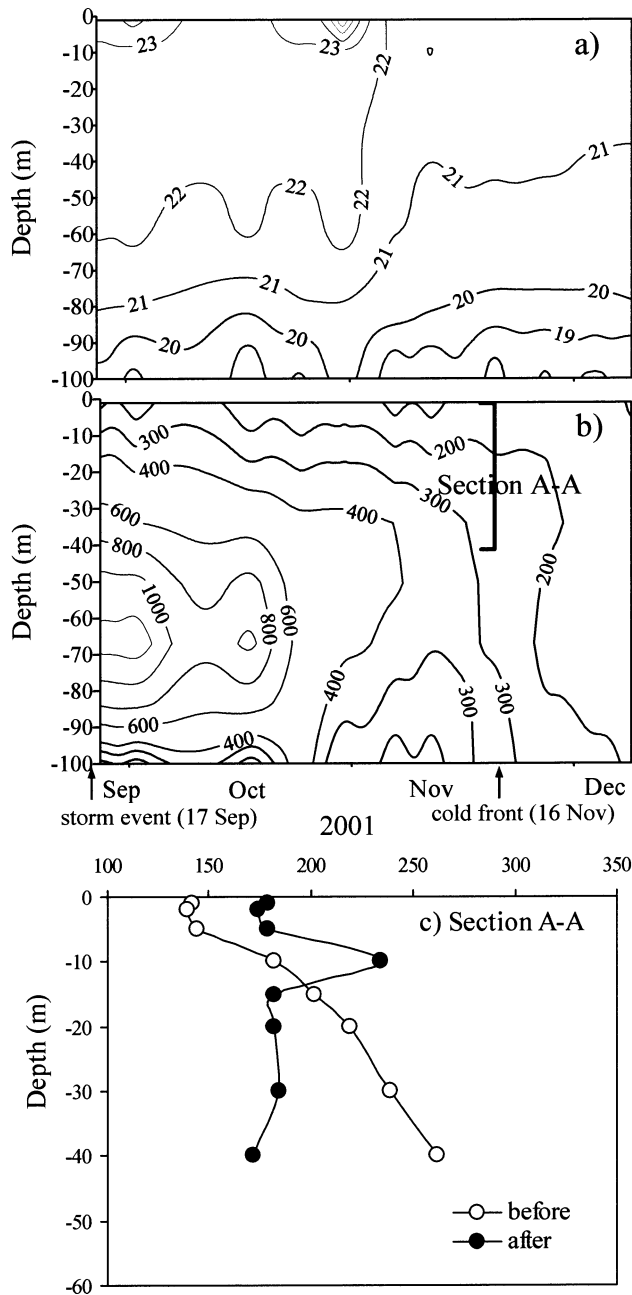To minimize the effects of excess suspended solids and

Fig. 6.   Isopleths of the (a) water temperature (°C) and (b) suspended solids (mg L^{-1}) at the dam. (c) The vertical distributions of concentrations of suspended solids between 0 and 40 m in depth (Section A-A) just before and after the cold front (16 November 2001). The sampling dates before and after the cold front were 12 November 2001 and 21 November 2001, respectively.

total phosphorus loading, the original No. 1 subsurface withdrawal (148 m asl) at a depth of 15 m was shut off and replaced by No. 3 withdrawal (108 m asl) at a depth of 55 m after the arrival of the storm events. Table 3 lists the estimated suspended solids withdrawal obtained by multiplying the outflow rate by the concentration of suspended solids behind the dam at the No. 3 withdrawal (Fig. 3) in 2 months, from 27 September to 20 November. There was no

storm during the monitoring period. The total amount of suspended solids removed by this procedure in the following 2 months after the storm was 1.871×10^8 kg (equivalent to a volume of 1.44×10^5 m³; Table 3). However, had withdrawal still been operational through No. 1, the total suspended solids removal would have been 5.805×10^7 kg (equivalent to 4.47×10^4 m³ by volume). This new strategy effectively removed 99,256 m³ of suspended solids by volume, which significantly prolonged the reservoir's storage capacity.

The excess suspended solids leaving the reservoir were transported continuously by gravity flow in a closed conduit to the water treatment plant. The peak measured suspended solids concentration at the entrance of the water treatment during the storms was 10,000 mg L^{-1}, which required a large dose of polyaluminum chloride to reduce turbidity to levels sustainable for drinking. Nevertheless, the fare of polyaluminum chloride used to treat this water at the treatment plant would be less costly than removal of sediments in the reservoir by dredging.

Effects on water quality—Suspension transported by the turbid density flow dissipated gradually after the flow's cessation and was eventually gone in 1 month. High concentrations of suspended solids occurred in the upper and lower water columns of the dam area; concentrations were lower in the intermediate depths (Fig. 3d). Concentration of suspended solids between the depths of 50 and 70 m was 1,078–1,621 mg L^{-1} on 8 October 2001 (10 d after the storms) and dropped to 301–717 mg L^{-1} on 31 October 2001 (33 d after the storms), whereas suspended solids below 80 m depth and above 40 m depth remained stable.

Similarly, total phosphorus was also high in the upper and lower water columns in the dam area after the storm (Fig. 5c). Another concern is the effect of high suspended solids concentration on the degree of transparency of the surface water. Figures 6a and b show the temporal variations of water temperature and suspended solids behind the dam. The incoming storm flow in September disrupted stable stratification. After reduction of the suspended solids by the subsurface withdrawal in October, the density of water was controlled mainly by the variation of the air temperature and heat loss from the surface, especially during the low flow periods in winter. When the cold front of 16–20 November 2001 occurred, air temperature fell to 13.9°C (Fig. 2); the entire body of water cooled to 21.2°C in the upper 40 m (Fig. 6a). The instability of the water body owing to the small density difference (0.2 kg m^{-3}) between 40 and 60 m, which was affected by the heat loss from the surface, caused vertical mixing of the water body. Large amounts of suspended solids originally within 40 m were mixed and redistributed, leading to lower concentration below 30 to 40 m and higher concentrations at shallower depths (Fig. 6c). The annual average value of the transparency (Secchi disk) in Feitsui Reservoir between 1996 and 2001 was 2.6–3.4 m. After the storm events in September 2001, the transparency of the surface water dropped to 1 m in October. In November, after the vertical mixing associated with a cold front, the transparency of the surface water decreased further to 0.5 m. Although high excess suspended solids loading was

reduced by adjusting the water intake depth, suspended solids transport still negatively affected the surface water quality through vertical mixing. To avoid this problem the location of subsurface withdrawal should be flexible, depending on continuous measurements of vertical water temperature, suspended solids, transparency, and nutrients.

References

ALAVIAN, V., G. H. JIRKA, R. A. DENTON, M. C. JOHNSON, AND H. G. STEFAN. 1992. Density currents entering lakes and reservoirs. J. Hydraul. Eng. **18:** 1464–1489.

ANNANDALE, G. W. 1987. Reservoir sedimentation. Elsevier.

CHEN, Y. J., AND S. C. WU. 2003. Effects of sediment phosphorus release associated with the density current on water quality of a sub-tropical and deep reservoir in Taiwan. Water Sci. Technol. **48:** 151–158.

———— AND ————. 2004. Effects of the phosphorus forms of the watershed on the speciation of phytoplankton: A case study of the two subtropical deep reservoirs in Taiwan. Proceedings of the ASCE EWRI 2004 World Water and Environmental Congress, Salt Lake City, UT.

CHIKITA, K. 1989. A field study on turbidity currents initiated from spring runoffs. Water Resour. Res. **25:** 257–271.

DALLIMORE, C. J., J. IMBERGER, AND T. ISHIKAWA. 2001. Entrainment and turbulence in saline underflow in Lake Ogawara. J. Hydraul. Eng. **127:** 937–947.

DE CESARE, G., A. SCHLEISS, AND F. HERMANN. 2001. Impact of turbidity currents on reservoir sedimentation. J. Hydraul. Eng. **127:** 6–16.

FORD, D. E., AND M. C. JOHNSON. 1983. An assessment of reservoir density currents and inflow processes. Technical report E-83-7, U.S. Army Corps of Engineering Waterways Experiment Station, Vicksburg, MS.

———— AND ————. 1986. An assessment of reservoir mixing processes. Technical report E-86-7, U.S. Army Corps of Engineering Waterways Experiment Station, Vicksburg, MS.

GILL, A. E. 1982. Appendix 3: Properties of seawater, p. 599–600. *In* A. E. Gill [ed.], Atmosphere-ocean dynamics. Academic Press.

HEBBERT, B., J. IMBERGER, I. LOH, AND J. PETTERSON. 1979. Collie River underflow into the Wellington Reservoir. J. Hydraul. Div., ASCE **105:** 533–545.

JIAHUA, F. 1986. Turbidity density currents in reservoirs. Water Int. **11:** 107–116.

KNELLER, B., AND C. BUCKEE. 2000. The structure and fluid mechanics of turbidity currents: A review of some recent studies and their geological implications. Sedimentology (suppl.) **47:** 62–94.

LAMBERT, A., AND F. GIOVANOLI. 1988. Records of riverborne turbidity currents and indications of slope failures in the Rhone delta of Lake Geneva. Limnol. Oceanogr. **33:** 458–468.

LUDLAM, S. D. 1974. Fayetteville Green Lake, NY. 6. The role of turbidity currents in lake sedimentation. Limnol. Oceanogr. **19:** 656–664.

MARTIN, J. L., AND S. C. MCCUTCHEON. 1999. Hydrodynamics and transport for water quality modeling. Lewis.

MURPHY, J., AND J. P. RILEY. 1962. A modified single solution method for the determination of phosphate in natural waters. Anal. Chim. Acta **27:** 31–36.

NIX, J. 1981. Contribution of hypolimnetic water on metalimnetic dissolved oxygen minima in a reservoir. Water Resour. Res. **17:** 329–332.

SAVENKO, V. S. 1999. Phosphorus discharge with suspended load. Water Res. **26:** 41–47.

SIMPSON, J. E. 1987. Gravity currents: In the environment and the laboratory. Cambridge University Press.

UUSITALO, R., M. YLI-HALLA, AND E. TURTOLA. 2000. Suspended soil as a source of potentially bioavailable phosphorus in surface runoff waters from clay soils. Water Res. **34:** 2477–2482.

WETZEL, R. G. 2001. Limnology—lake and river ecosystems. Academic.

YU, W. S., H. Y. LEE, AND S. H. M. HSU. 2000. Experiments on deposition behaviour of fine sediment in a reservoir. J. Hydraul. Eng. **126:** 912–920.